PHYSICAL REVIEW B VOLUME 59, NUMBER 12 15 MARCH 1999-II

Diffusion and transient trapping of metals in silicon

J. Wong-Leung and J. S. Williams
Department of Electronic Materials Engineering, Research School of Physical Sciences & Engineering, The Australian National University, Canberra, ACT 0200, Australia

A. Kinomura
Osaka National Research Institute, AIST, 1-8-31 Midorigaoka, Ikeda, Osaka 563-8577, Japan

Y. Nakano and Y. Hayashi
Research Reactor Institute, Kyoto University, Kumatori-cho, Sennan-gun, Osaka 590-0494, Japan

D. J. Eaglesham
Bell Laboratories, Lucent Technologies, 600 Mountain Avenue, Murray Hill, New Jersey 07974
(Received 8 September 1998)

In this study, the transport of ion-implanted metals to cavities and subsequent metal dissolution have been examined for short- and long-annealing times using Rutherford backscattering and channeling, transmission electron microscopy, and neutron activation analysis. A band of nanocavities in Si is found to be a very efficient sink for implanted Au and Cu during short-time annealing. In this case, the system appears to be in pseudoequilibrium where the fraction of soluble metals is well below the expected solubility even when bulk phase (silicide) is present. However, long-term annealing results in dissolution of metals and progression towards thermal equilibrium solubilities. We suggest that the slow equilibration is a result of both the local metal supersaturation and disorder resulting from implantation. The role of defects (particularly Si interstitials) in both the transient and slow equilibration processes is discussed. For example, metal transport and trapping at cavities are defect mediated processes and subsequent dissolution can also be defect limited.
[S0163-1829(99)10011-0]

I. INTRODUCTION

With the reduction of device dimensions, there is a need to reduce concentrations of metals in Si to well below their equilibrium solubilities at present processing temperatures. Metals inadvertently introduced during processing are fast diffusers and can accumulate in active device regions, causing dramatically reduced device performance. Metals can be removed from active device regions by the introduction of so-called gettering layers, which are regions of preferential accumulation of metals. It is crucial to understand the mechanisms of metal gettering to such layers where the transport is largely influenced by the diffusivity and solubility values[1] of different metals in Si. Most gettering processes, at equilibrium, are believed to take place through one of two main mechanisms.[2] Relaxation-induced gettering requires a supersaturation of the metallic impurities in the bulk of the wafer and favorable nucleation/precipitation sites in the gettering layer. Such a supersaturation is achieved during cooldown as a result of the strong temperature dependence of the solubility limit of metals in Si, thus providing a strong driving force for fast-diffusing metallic impurities to accumulate and locally precipitate at favorable trapping sites in the getter layer.[2] Such a process requires that the cooling rate is sufficiently slow so as to facilitate long-range metal transport to the getter layer during cooling. In contrast, segregation-induced gettering does not require a supersaturation of metals in the wafer. In this case, gettering is due to enhanced solubility or new compound formation in the gettering layer, thus resulting in a new equilibrium partitioning of metals in the bulk and the getter layer, which can dramatically reduce the bulk concentration at all temperatures in equilibrium. Such a gettering mechanism is more suitable to the needs of the device industry, which is aiming at levels of metallic impurities $<10^{10}\,\mathrm{cm}^{-3}$,[3] far below the solubility levels of metals in Si at processing temperatures of 600–950 °C.

The above gettering processes occur in thermodynamic equilibrium. It is debatable as to whether such mechanisms can still be valid in cases where the gettering layer has been generated by ion implantation, thereby providing a local supersaturation of metal and a high concentration of defects, which together constitute a decidedly nonequilibrium situation. If metals are introduced by ion implantation, even at implantation doses as low as $10^{13}\,\mathrm{cm}^{-2}$, a substantial metal supersaturation is obtained and considerable implantation damage results. In such cases, the gettering process can indeed be dominated by nonequilibrium processes with the interaction of implantation-induced defects playing a dominant role.

Au is a case where the availability of defects plays a crucial role in diffusion and solubility even under equilibrium situations. Au diffuses by continuously sampling substitutional (Au_s) and interstitial (Au_i) sites. Its substitutional solubility is much higher than its interstitial solubility. However, there are two mechanisms proposed for Au transport, namely, the Frank-Turnbull mechanism[4] and the kick-out mechanism[5–8] represented by Eqs. (1) and (2), respectively.

 ©1999 The American Physical Society

TABLE I. Table comparing the substitutional and interstitial solubilities of different metals at different temperatures quoted from Ref. 1.

Species	Dose (cm^{-2})	Annealing temperature 1 hr (°C)	Amount of metal gettered (cm^{-2})	Corresponding concentration of metals if equilibrated throughout the wafer (cm^{-3})	Solubility level (cm^{-3})
Au	8×10^{13}	850	8×10^{13}	1.6×10^{15}	2×10^{15}
Cu	6×10^{14}	780	6×10^{14}	1.2×10^{16}	4.2×10^{16}
Au	9.2×10^{14}	950	9×10^{14}	≈50% above sol. limit	9.2×10^{15}
Cu	2.2×10^{15}	780	*1.9×10^{15}	at sol. limit	4.2×10^{16}

*at surface and cavities.

$$Au_i + V \rightleftharpoons Au_s \quad (1)$$

$$Au_s + Si_i \rightleftharpoons Au_i, \quad (2)$$

where V and Si_i represent vacancies and Si interstitials, respectively. When Au is diffused into Si, it is known to exhibit a characteristic U-shaped profile with high concentrations of Au at both surfaces, which act as strong sinks for Si interstitials. The Au concentration in the middle of the U-shape profile increases with the square root of time, a characteristic that is best explained by the kick-out formalism whereby the rate at which Au goes substitutional in the bulk of the wafer is limited by the slow removal of excess Si interstitials. Thus, the equilibration of Au in Si is much slower than would be expected based on the product of (interstitial) diffusivity and (substitutional) solubility due to the slow removal of Si interstitials from the bulk of the wafer. Further studies[6–8] on Au diffusion in highly dislocated regions in Si clearly show that dislocated regions are also strong sinks for Si interstitials and can give rise to W-shaped Au profiles. Those studies clearly show the influence of strong sinks on both the Au profile and the effective diffusion rate. Cu diffusion is believed to be less complex in nature. The interstitial solubility of Cu is much higher than the substitutional solubility and because of its high-interstitial diffusivity, Cu predominantly diffuses interstitially and remains in interstitial sites: it does not require point defect interaction or defect removal for equilibration.[1] Consequently, such differences between Au and Cu should be important in understanding gettering mechanisms in the ion-implanted case where high concentrations of defects are present and the system is initially far from equilibrium.

This study aims at understanding the gettering behavior of ion-implanted metals to cavities in Si. Our results clearly indicate a complex gettering mechanism where metal-defect interactions seem to play a crucial role. Initially, essentially all the implanted Cu and Au can be gettered to cavities at processing temperatures with the amount of metals in solution being extremely low. However, long-time annealing results in partial release of metal from cavities and the establishment of an apparent equilibrium situation. This long equilibration process appears to be limited (for both Au and Cu) by nonequilibrium defect-mediated processes.

II. EXPERIMENT

In the various experiments, both Czochralski (Cz) and float-zone (FZ) Si wafers of (100) orientation were used as indicated below. However, the qualitative behavior of the initial transient gettering stage and the final equilibration process are the same, independent of whether FZ or Cz wafers are used. For some of the equilibration experiments, some FZ wafers polished on both sides were used thereby reducing the possibility of a competition with backside gettering due to mechanical damage.

Si wafers were implanted with either (a) 50 keV or (b) 100 keV H^- to a dose of $3\times10^{16}\,cm^{-2}$ at room temperature. The damage generated by these two implants was preannealed at 850 °C for 1 hr to form a band of nanocavities at depths 0.6 μm and 1.0 μm, respectively.[9] The depth of the cavities was chosen carefully to allow quantitative analysis of the different metals at the cavities by Rutherford backscattering (RBS). The Cu signal at depths greater than 0.8 μm is hidden by the Si edge when analyzed by a 2-MeV He beam with the detector at an angle of 168° from the direction of incidence. The metals were introduced in the near surface of the wafers by ion implantation, which allows the metal concentration to be adjusted with respect to the solubility level of the respective metals in Si at the processing temperature. For instance, a 70-keV Cu implant to a dose of $6\times10^{14}\,cm^{-2}$ and a 95-keV Au implant to a dose of $8\times10^{13}\,cm^{-2}$ at room temperature were chosen for experiments requiring concentrations of metals throughout the wafers, which are below the respective solubilities at 780 °C and 850 °C (see Table I). On the other hand, a Au dose of $1\times10^{15}\,cm^{-2}$ would be an amount of Au well above the amount expected to go into solution at 950 °C.

The anneals in this study were all performed under flowing Ar gas in conventional quartz tubes. The annealing temperatures were chosen based on the diffusivity and other properties of Cu and Au in Si. Consequently, for equilibration experiments, annealing temperatures of 950 °C were used for Au experiments. For Cu, long-annealing treatments were carried out at 780 °C for 24 hr. In this case, the annealing temperature was not increased above 800 °C in order to minimize any possibility of Cu evaporation.[10] The samples were usually removed from the hot zone of the furnace such that the temperature dropped to below 500 °C in a few seconds.

RBS was the main quantitative method of measuring the metal profiles and checking the implanted dose while cross-sectional transmission electron microscopy (XTEM) allowed the characterization of the microstructure of the samples. With these techniques, low concentrations of soluble metals cannot be detected. As a result, neutron activation analysis (NAA) was performed to determine the absolute amount of metals present in the wafers and, together with appropriate

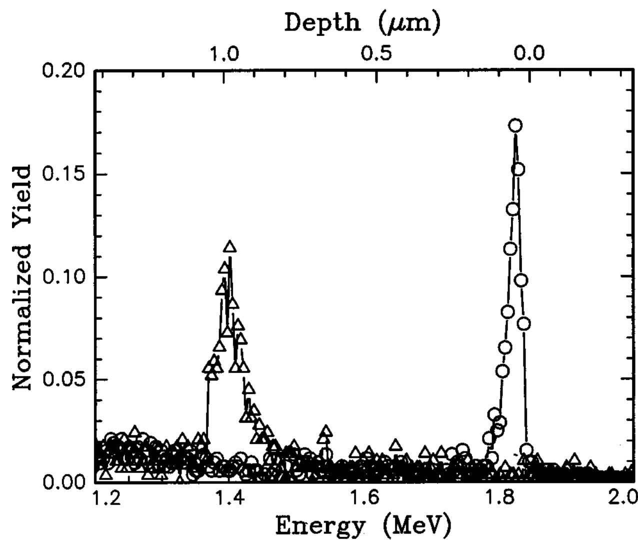

FIG. 1. RBS-*R* spectra showing the distribution of Au in samples containing H-induced defects preannealed at 850 °C for 1 hr prior to a Au implant to a dose of $8\times10^{13}\,\mathrm{Au\,cm^{-2}}$, (○) as-implanted and (△) annealed at 850 °C for 2 hr.

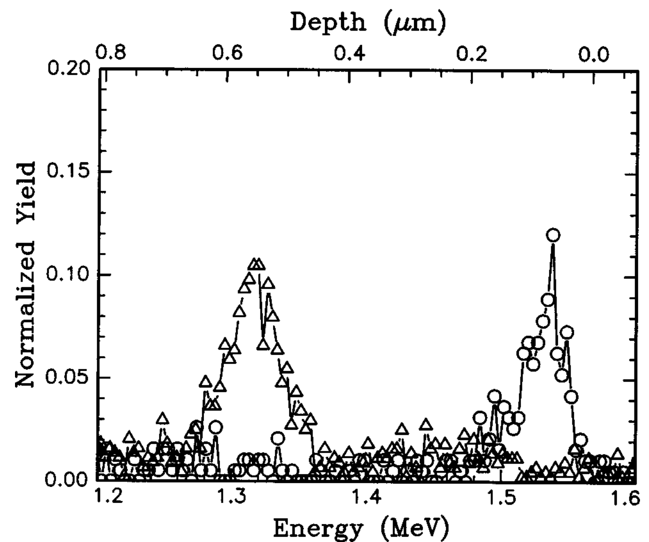

FIG. 2. RBS-*R* spectra showing the distribution of Cu in samples containing H-induced defects preannealed at 850 °C for 1 hr prior to a Cu implant to a dose of $7\times10^{14}\,\mathrm{cm^{-2}}$, (○) as-implanted and (△) annealed at 780 °C for 1 hr.

etching techniques, allowed the measurement of the absolute amount of metals present in the bulk of the wafers. The NAA measurements were carried out at the Kyoto University Reactor. Samples (in this case, high-quality Fz wafers were used in order to keep the background counts low) were irradiated for 206 hr in the core irradiation facility with a nominal thermal neutron flux of $4.7\times10^{13}\,\mathrm{n/cm^2\,s}$. Gamma rays from the irradiated samples were measured about 4 and 11 days after the end of irradiation by a pure Ge detector. Au densities were calculated from a gamma-ray peak at 411.8 keV caused by the $^{197}\mathrm{Au}(n,\gamma)\,^{198}\mathrm{Au}$ decay reaction. The surfaces of samples, including the cavity layers, were etched off by a mixture of HNO_3 and HF, followed by an aqua regia clean (a mixture of HCl and HNO_3). Etched depths calculated from weight loss were about 30 μm. Gamma-ray yields were measured before and after etching to determine the location of the Au.

In order to assess the effect of cavities on the equilibration expected for the different metals and annealing conditions, appropriate control samples were prepared by performing similar annealing treatments on plain Cz Si wafers subject to similar metal implants.

III. EXPERIMENTAL RESULTS

Figure 1 shows the typical RBS profiles of Au in a Cz Si wafer with preformed cavities and $8\times10^{13}\,\mathrm{Au\,cm^{-2}}$. Clearly, a 2-hr anneal at 850 °C relocates almost all of the implanted Au to the cavity band with very little Au in solution in the wafer. Our previous XTEM studies have shown that the cavities created under these conditions have an internal surface coverage close to $1\times10^{14}\,\mathrm{cm^{-2}}$.[9] Hence, we expect that a Au dose of $8\times10^{13}\,\mathrm{cm^{-2}}$ will decorate the cavities at close to a monolayer coverage and is insufficient to form Au precipitates at the cavities. The RBS profiles for Cu indicate a similar behavior. As shown in Fig. 2, in similar samples with cavities and a Cu dose of $6\times10^{14}\,\mathrm{cm^{-2}}$, most of the implanted Cu was driven to the cavities after a 1-hr anneal at 780 °C. This Cu dose is well above a monolayer coverage on the cavity walls and results in bulk-phase precipitation at the cavities.[9] In both the Au and Cu cases, the total amount of metal measured by RBS is essentially the same after annealing as before with little apparently in solution. These two results clearly indicate that the amount of metals in solution in the wafers is well below their known equilibrium solubilities in Si (e.g., Table I), independent of their widely different diffusivities.

A key question is whether equilibration of the metals has been achieved in the cases discussed above or equilibration is limited by metal-defect interactions and complex diffusivity. Hence, longer annealing time experiments were designed. Fz Si wafers polished on both sides were used in the equilibration experiments. For NAA measurements, high grade Fz Si wafers of (100) orientation were implanted with 100-keV H and annealed at 850 °C for 1 hr to preform the cavities. 95-keV Au was implanted into the wafers to a dose of $3\times10^{13}\,\mathrm{cm^{-2}}$. The samples were annealed at 950 °C for 1 hr to drive the Au to cavities. Long-annealing treatments were carried out at 950 °C for 24 hr on these and other samples implanted with Au doses below $10^{14}\,\mathrm{cm^{-2}}$. Typical results are summarized in Fig. 3, the open circles in Fig. 4 and in Table II. In Figs. 3(a), 3(b), and 3(c), the peaks indicated by arrows are gamma-ray emissions arising from the activation of Au. After annealing at 850 °C for 1 hr, according to the RBS results (Fig. 1), the implanted Au is relocated to the cavities without significant ''loss'' of Au. An etch of the near surface region should remove most of the implanted Au. In the NAA spectra, Fig. 3(b), the peaks corresponding to Au were lowered by more than an order of magnitude compared to the as-implanted spectrum, showing that most of the Au is at the cavities, with very little Au in solution in the wafer after the 1-hr anneal at 850 °C. This is in agreement with the RBS results previously discussed and shown in Fig. 1 and with the cavity sample in the lower part of Fig. 4. Note that the as-implanted Au doses in Fig. 4 measured by RBS are not exactly the same for samples with cavities and samples without cavities. However, the trends for annealed

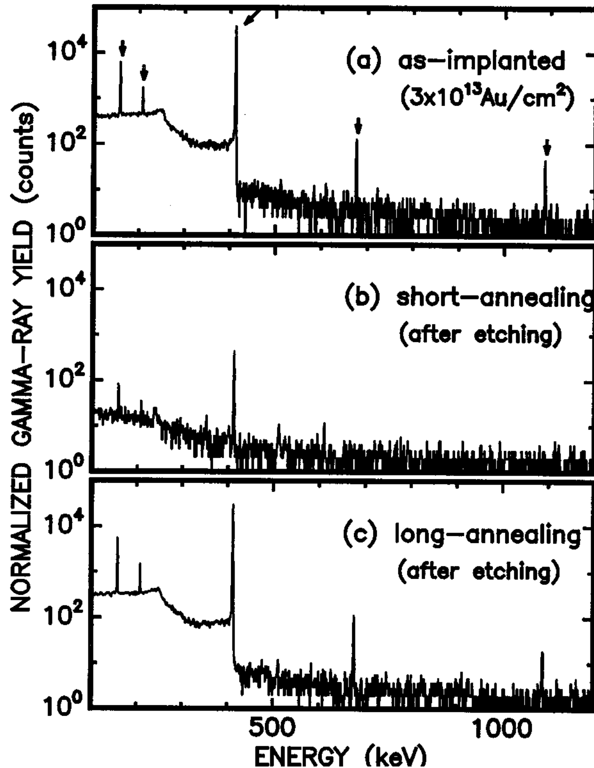

FIG. 3. Neutron activation analysis spectra from samples containing cavities and 3×10^{13} Au cm^{-2}: (a) as-implanted, (b) after 1-hr anneal at 850 °C and etched by HNO_3/HF solution and aqua regia, (c) 1 hr at 850 °C, 24-hr anneal at 950 °C and etched by HNO_3/HF solution and aqua regia.

samples are clear. The results for the control sample (without cavities) also show that a short anneal results in most of the Au being retained in the implanted damage region, with again only a small amount of Au in solution. However, after the samples were annealed for 24 hr at 950 °C, the RBS analysis showed no Au peaks at the cavities or at the surface for samples both with and without cavities, as shown in Fig. 4 where the Au concentration is below the detection limit

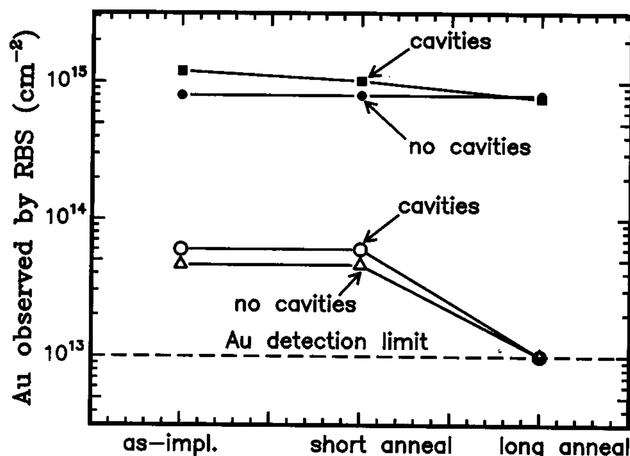

FIG. 4. Graph showing the amount of Au detected by RBS in samples with and without cavities after different annealing treatments: at surface for samples without cavities, at cavities and surface for samples with cavities.

($\approx10^{13}\,cm^{-2}$). However, the NAA spectrum of low-dose samples confirmed that all the implanted Au remained in the sample after the long anneal, with no evidence for Au evaporation. The quantitative NAA results are summarized in Table II. After a short anneal, essentially all the implanted Au is trapped at cavities or the surface but after a long anneal, the Au is released into solution throughout the bulk.

It is interesting to examine the behavior for high-dose Au, which exceeds the solubility limit when distributed throughout the wafer. With a Au implant dose close to $1\times10^{15}\,cm^{-2}$, a 1-hr anneal at 850 °C results in the relocation of most of the implanted Au from the surface to the cavities as shown in the RBS spectra in Fig. 5. Figure 4 (filled symbols) shows that short-time annealing of samples with and without cavities results in the accumulation of essentially all the Au at cavities or within implant damage, respectively. Previous XTEM investigation of samples with similar coverage of Au at the cavities after a 1-hr anneal at 850 °C showed the decoration of the internal surfaces of well-faceted cavities with the nucleation of Au precipitates at the cavity band.[11] A typical micrograph of this sample is illustrated in Fig. 6(a). However, after the sample with cavities is subjected to a long, high-temperature annealing treatment, we observe a substantial decrease in the amount of Au at the cavities, as shown in Figs. 4 and 5. It is interesting to note that the decrease in the amount of Au, if distributed throughout the wafer, corresponds to a concentration ($8.1\times10^{15}\,cm^{-3}$) close to the solid solubility limit of Au in crystalline Si at 950 °C ($9.2\times10^{15}\,cm^{-3}$).[1] Although, RBS cannot detect such a low concentration of Au in bulk Si our anneal conditions are consistent with those previously used[12] to achieve a uniform Au distribution throughout a Si wafer up to the solid solubility limit. XTEM examination of the Au sample with cavities after the long anneal [Fig. 6(b)] revealed a dramatic evolution of the microstructure. Prior to the long anneal, few strain fields and dislocations were observed close to the depth of the cavity band [Fig. 6(a)]. After the long anneal, empty cavities are not observed and the Au precipitates have grown larger at the expense of the smaller ones. In some parts of the sample, the precipitates appear to have migrated closer to the surface thus extending its distribution over a much larger distance. In such cases, the precipitates were often pinned to well-defined, long dislocation lines. XTEM observations indicate that such cases do not dominate the microstructure of the sample and this is in agreement with the RBS spectrum in Fig. 5, where the positions of the Au profile at the cavities before and after the long-annealing treatment are identical. Also shown in Fig. 4 (filled circles) is the case of long-time annealing of a sample without cavities. In this case, little Au goes into the solution but a dramatic Au-enhanced oxidation of the surface (to a depth of around 1000 Å) was observed despite the fact that the samples were annealed in Ar. This enhanced oxidation has been reported previously[13] and this process appears to inhibit the dissolution of Au. No oxidation was observed in samples with cavities and little Au was retained at the surface.

With reference to the low-dose Cu (below the solid solubility level) we can also track the behavior of implanted Cu during short- and long-annealing times at 780 °C. The results are summarized in Fig. 7 (open symbols) for a Cu dose of

TABLE II. Summary of the amounts of Au detected by NAA in the different samples.

Sample	Before etching: Areal density (Au/cm^2)	Before etching: Concentration (Au/cm^3)	After etching: Areal density (Au/cm^2)	After etching: Concentration (Au/cm^3)
Short annealing	4.8×10^{13} ($\pm 0.88 \times 10^{13}$)	1.3×10^{15} ($\pm 0.16 \times 10^{15}$)	5.4×10^{11} ($\pm 1.0 \times 10^{11}$)	1.7×10^{13} ($\pm 0.23 \times 10^{13}$)
Long annealing	4.8×10^{13} ($\pm 0.88 \times 10^{13}$)	1.3×10^{15} ($\pm 0.17 \times 10^{15}$)	3.9×10^{13} ($\pm 0.72 \times 10^{13}$)	1.2×10^{15} ($\pm 0.16 \times 10^{15}$)

$3.4 \times 10^{14}\,\mathrm{cm}^{-2}$ into samples with and without cavities. During the short-time (1-hr) anneal, all of the Cu is trapped at cavities, or in the implant damage region for the sample without cavities. In the latter case, a small amount (≈10%) of Cu may be in solution but, in the case of the cavity sample, all the Cu is located at cavities. However, after a subsequent anneal for 24 hr at 780 °C, Cu has clearly dissolved. In the case of the sample without cavities, essentially all Cu is now in solution (within the detection limit of RBS) whereas the sample with cavities has $2 \times 10^{14}\,\mathrm{Cu\,cm}^{-2}$ still residing at the cavities despite the fact that the amount of Cu in solution is still well below the solubility limit. Possible explanations for this behavior are given in Sec. IV.

In the case of high-dose Cu (above the solubility limit), RBS analysis as shown in Fig. 8 showed that more than 90% of the implanted Cu either diffused to the cavities or was retained at the surface after the first anneal. XTEM examination in Fig. 9(a) indicates the presence of bulk-phase Cu at the cavities, as shown by the moiré fringes, consistent with our previous reports.[9] Figure 7 summarizes the high-dose Cu behavior for two Cu doses above $10^{15}\,\mathrm{cm}^{-2}$ into a sample with cavities and one without. In the case of the sample without cavities almost 30% of the Cu appears to go into solution during 1 hr at 780 °C with the remainder trapped within the implant damage region. RBS analysis of the samples subjected to the long-annealing treatment (see Figs. 7 and 8) indicates a loss in the amount of Cu located at the cavities. Again, the decrease in the amount of Cu at the cavities detected from RBS is consistent with the solubility values of Cu at 780 °C. The amount of Cu undetected by RBS, if distributed uniformly throughout the whole wafer, corresponds to a concentration ($2.5 \times 10^{16}\,\mathrm{cm}^{-3}$) close to the solubility value of Cu at 780 °C ($4.2 \times 10^{16}\,\mathrm{cm}^{-3}$). This is a very surprising result since one would expect, from the known diffusivity and solubility values of Cu at 780 °C,[1] that Cu would equilibrate throughout the bulk of the wafer within 20 s. Thus, Cu should have equilibrated during the short (1 hr) anneal at 780 °C. In contrast to the Au case, XTEM examination [see Fig. 9(b)] indicated that the microstructure of the

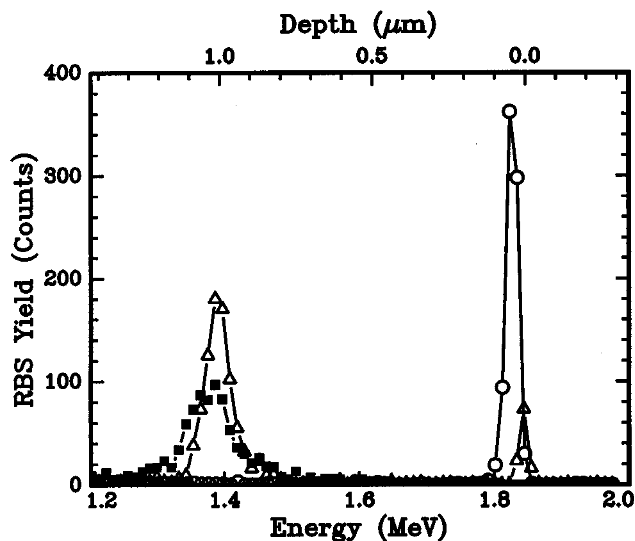

FIG. 5. RBS-*R* spectra showing the Au profile in samples as-implanted with H and Au ($1 \times 10^{15}\,\mathrm{cm}^{-2}$) (○), then annealed at 850 °C for 1 hr (△) and finally reannealed at 950 °C for 48 hr (■), respectively.

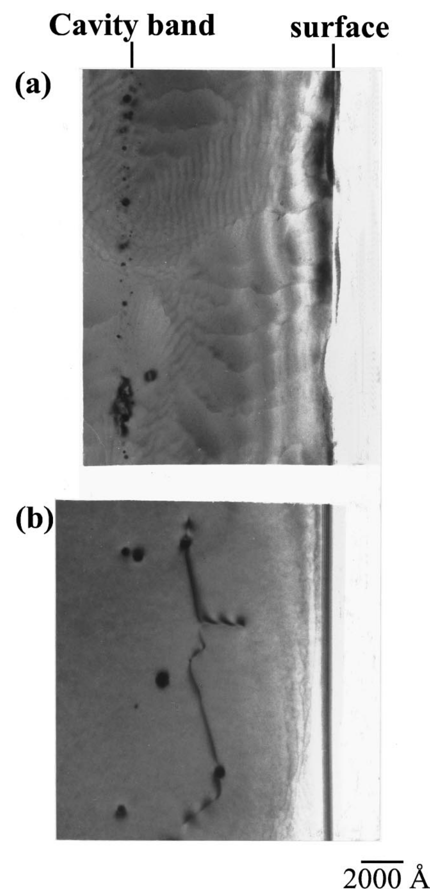

FIG. 6. XTEM micrograph of Si implanted with H and Au ($1 \times 10^{15}\,\mathrm{cm}^{-2}$) (a) after 1-hr anneal at 850 °C and (b) a further 48-hr anneal at 950 °C.

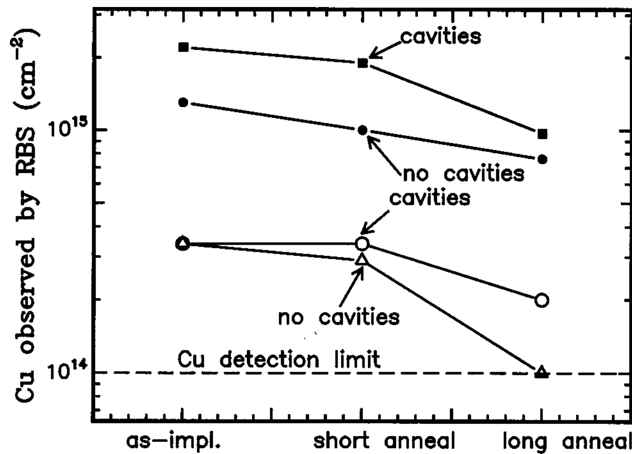

FIG. 7. Graph showing the amount of Cu detected by RBS in samples with and without cavities after different annealing treatments: at surface for samples without cavities, at cavities and surface for samples with cavities. The measured as-implanted Cu doses are not the same for samples with cavities and those without cavities.

sample changed very little during the long-annealing treatment, i.e., the size and the density of cavities, the size of bulk-phase Cu precipitates did not change. This is probably due to the fact that in the Cu case the long-annealing treatment was performed at the same temperature as the initial anneal to drive Cu to the cavities. The size and shape of the cavities induced by He implantation has been previously shown to be largely dependent on the annealing temperature,[14] with the equilibrium shape being reached after 1 hr annealing.

IV. DISCUSSION

One of the most interesting (and surprising) results in this study is the initial accumulation, during short-time annealing, of essentially all the Au and Cu to either implantation damage or to a cavity band. During this process, only a small fraction of the metals appear to be in solution at the annealing temperature. As indicated earlier, this might be expected for Au, which requires long-annealing times and the removal of excess Si interstitials before uniform substitutional solubility can be attained.[1] However, for Cu, a 1-hr anneal at 780 °C might be expected under equilibrium conditions, to result in Cu dissolution up to its solubility limit. Our observations indicate that such Cu dissolution does not occur for the following reasons. First, if we assume that Cu dissolves up to its equilibrium solubility limit at the annealing temperature, based on literature solubilities and diffusivities for Cu in Si between 500 °C and 800 °C, we would expect less than about 5×10^{13} Cu cm^{-2} to accumulate at cavities from relaxation gettering during our relatively rapid quench (N.B. This calculation is based on our quenching rate being able to cool this sample to below 500 °C in a few seconds). However, we observe essentially all of the implanted Cu either at the surface or cavities following annealing. Second, we unequivocally demonstrated previously, by hot RBS measurements, that implanted Cu accumulates at cavities during annealing. Consequently, our short-time annealing results indicate that the implant (near surface) damage and a cavity band are initially strong sinks for diffusing metals, with little tendency for metals to dissolve. In this situation, Si containing surface damage or a band of cavities can be considered

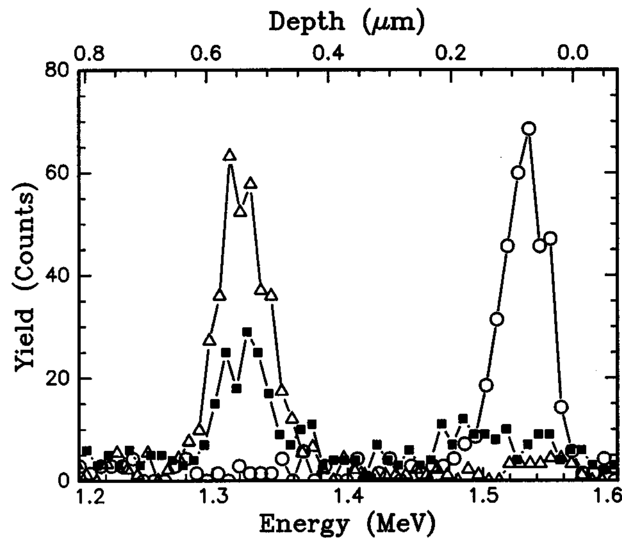

FIG. 8. RBS-*R* spectra showing the distribution of Cu in samples implanted with both H and Cu, (○) as-implanted, (△) annealed at 780 °C for 1 hr, (■) annealed at 780 °C for 1 hr and reannealed at 780 °C for 24 hr.

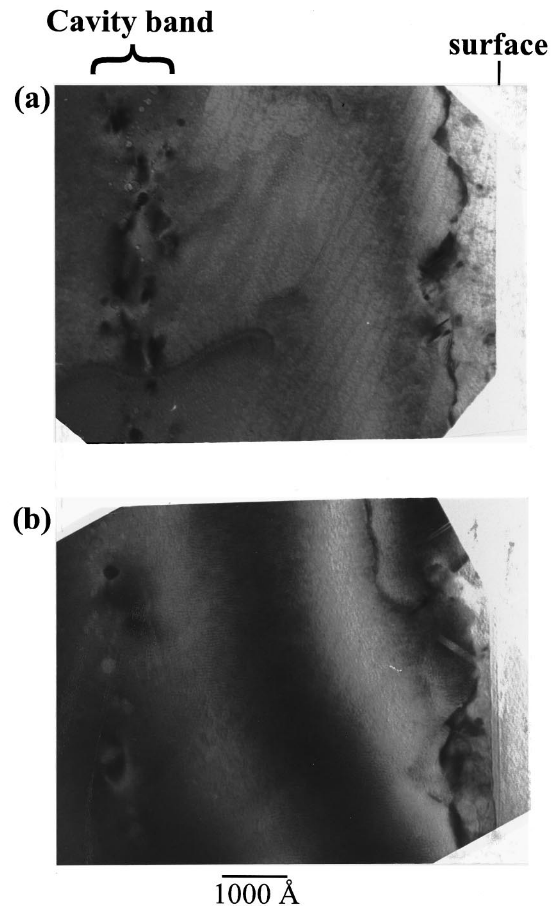

FIG. 9. XTEM micrograph of Si implanted with H and Cu (2.2×10^{15} cm^{-2}) (a) after 1-hr anneal at 780 °C and (b) a further 24-hr anneal at 780 °C.

far from thermodynamic equilibrium. The system appears to achieve a ''pseudoequilibrium'' with very low Cu solubility, in competition with strong sinks for diffusing interstitials and even bulk (silicide) phase if the overall metal concentration is sufficiently high. In this metastable state, with implantation damage and cavities, a new pseudoequilibrium partitioning may result.

For the short-time anneals, the comparison between the results for samples with and without cavities is interesting. We note that the introduction of metals by ion implantation leads to a local, very large supersaturation of metal within a heavily damaged region. There is thus a strong driving force for local precipitation during annealing in competition with diffusion away from the implanted region. Without cavities, we find that the metal atoms are totally trapped within the implant damage region even in high-dose cases where bulk phase is observed. However, when a cavity band is present, essentially all of the metals are transported to cavities where bulk phase is again observed for sufficiently high doses. Therefore, there is a competition between trapping and bulk-phase formation of metals at surface damage and at cavities. In the ''pseudoequilibrium,'' metastable situation achieved during short-time annealing, a balance (or new partitioning) exists between the fractions of metals in bulk phase, trapped at appropriate sites and a small amount in solution. Thus, in the presence of strong sinks, the fraction of soluble metal (both Au and Cu) can be well below the thermodynamic equilibrium value as illustrated in Fig. 10.

In terms of the long-time annealing behavior where both Au and Cu appear to dissolve into solution, let us consider the Au case first. According to the diffusivity and solubility values of interstitial Au at 850 °C, the diffusion length of Au for 2 hr at 850 °C is ≈ 1750 μm (the case for Fig. 1) and about 5 hr is required to redistribute $8\times10^{13}\,\mathrm{Au\,cm^{-2}}$ from the surface to the back of the wafer. However, previous data[12] in the Au-Si system have shown that annealing treatments at 950 °C for more than 20 hr are required to attain uniform solubility of Au through the wafer. Such slow equilibration behavior has previously been attributed to a complex diffusion process for Au in Si, where the effective diffusivity is quite low[5,12] and determined by the removal rate of Si interstitials.

Thus, the slow equilibration of Au is likely to be a result of the complex diffusion of Au and the conversion of Au from interstitial sites into substitutional sites. However, the oxidation of the internal surfaces of the cavities is equally likely to be another factor affecting the release of Au from the cavity band. Gao *et al.*[15] recently reported the oxidation of the internal surfaces of cavities after a two step anneal with the final one at high temperature ($\approx$1180 °C) under a N ambient. The presence of a thin shell of amorphous oxide was attributed to internal oxidation resulting from the presence of oxygen in Cz wafers. Such an oxide has not been characterized in our samples and the relative contributions of different processes to Au dissolution are currently under study. However, we note that, in our case, the dissolution of Au from cavities was observed both in Cz and Fz Si wafers where the concentration of O differs by two orders of magnitude. Thus, although internal oxidation may play some role in the slow dissolution process, it is unlikely to be the primary reason. In this context, it is interesting to compare the long-time annealing behavior of high- and low-dose Au cases.

The evolution of the microstructure of the high-dose Au sample during the long anneal involves a reduction in the number of ''empty'' cavities in favor of Au (or Au-Si eutectic) precipitates. Also, there is a growth in the size and a local migration of some of the Au precipitates. In this latter case, molten Au precipitates and their possible zone migration might have arisen as a result of the high-temperature gradients in the sample created during the heating-up and cool-down stages. Indeed, the movement of such molten precipitates has previously been observed[16] to leave tracks decorated with Au. The Ostwald ripening process contributes to growth of Au precipitates and is a process known to result in a reduction in the free energy of the system.

In the low-dose Au case, Au does not form bulk phase and decorates the internal surfaces of the cavities. In this situation, it is harder to explain why the Au dissolves from the cavities if strong Au-Si binding[17] at cavity walls persists following long-time annealing. However, Fig. 6 suggests that Au-decorated (''empty'') cavities may not survive a long anneal at 950 °C. This possibility and/or the passivation of the internal surfaces of the cavities at 950 °C might explain the eventual dissolution of low-dose Au from cavity walls. Further experiments need to be done to clarify this situation.

Although the complex, defect-mediated diffusion of Au might account for the slow equilibration of Au, such a reason cannot account for similar behavior for Cu in Si. Simple calculations using the product of the diffusivity and the solubility values of interstitial Cu at 780 °C indicate that $6\times10^{14}\,\mathrm{cm^{-2}}$ of Cu can be transported from the surface to a depth of 0.5 μm within 0.02 s and to the back of the wafer within 15 s. Thus, one would expect Cu to equilibrate (under thermodynamic equilibrium conditions) after such an annealing treatment. Yet, for all doses of Cu in this study, we observe very little Cu in solution after a 1 hr anneal at 780 °C: like the case of Au, the Cu is either trapped at the surface implant damage or at the cavities. Furthermore, Cu is observed to form bulk phase (at cavities) and it is therefore all the more surprising that the Cu is slow to dissolve. Again, we can argue that a new ''pseudoequilibrium'' partitioning is established between concentrations of Cu trapped at disorder and on cavity walls, in bulk phase and in solution. In such cases, the Cu solubility, in competition with Cu trapped (at cavities and disorder), is orders of magnitude lower than the solubility at thermal equilibrium. However, after longer-time annealing, Cu does dissolve and the system appears to move towards thermodynamic equilibrium. Why does this happen?

In attempting to explain the slow dissolution of Cu, we note that in all cases in this study we have both bulk phase Cu and Cu trapped at disorder (and cavity walls) after short-time annealing. Indeed, the tendency for a supersaturated Cu implant dose to precipitate as Cu_3Si is strong during annealing. Hence, there is a competition between silicide formation and Cu diffusion away from the high implant region during the initial stages of annealing. Once a silicide forms during this transient process, it must dissolve for Cu to diffuse. However, as pointed out in Ref. 18, an excess of Si interstitials will help the dissolution of Cu_3Si as the formation of Cu_3Si is accompanied by emission of Si interstitials. Indeed, we have previously shown that the silicide formation process

can inhibit the extent of Cu diffusion and gettering to cavities.[19] The fact that the cavities are strong sinks for Si interstitials will favor the silicide reaction rather than its dissolution. Thus, the slow equilibration of Cu may indeed be a result of the slow dissolution of Cu from silicide in cavities and/or in surface damage and the key role of Si interstitials in this process. The fact that Ostwald ripening does not occur for Cu-filled cavities, is presumably a result of the lower annealing temperature compared with the Au case. In addition, Cu trapped at disorder may be stable only as long as the disorder persists. Long-annealing times at 780 °C may begin the annealing out of disorder and the corresponding generation of Si interstitials may lead to the slow dissolution of Cu_3Si. Thus, we suggest that the slow equilibration of Cu is dominated by disorder and the role of defects in trapping and dissolution processes. The time taken for the system to achieve thermal equilibrium is determined by the operative rate-limiting defect interaction process.

At 780 °C, the residual Cu left at cavities following long-time annealing is about $2\times10^{14}\,\mathrm{cm}^{-2}$ (Fig. 7). This may suggest that this amount of Cu remains strongly bound to cavities and has little tendency to dissolve. Indeed, Myers, Follstaedt, and Bishop[20] have indicated that the driving force for the diffusion of Cu to cavities is the strong bonding sites provided by the internal walls of the cavities. In such a case, we might expect the Cu to accumulate to about 1 monolayer or roughly equivalent to the number of Si atoms occupying the internal surfaces of cavities. Previously, we have established the density of Si atoms on the cavity walls to be around $1\times10^{14}\,\mathrm{cm}^{-2}$ of sample for our 850 °C preanneal conditions. It is possible that long-time annealing causes a stable Cu-Si surface structure at the internal cavity walls which contains more than a monolayer of Cu. Alternatively, Cu may have accumulated at the cavities during quenching and may explain the amount of Cu accumulated in excess of the monolayer coverage at strong bonding sites at the internal cavity walls. We reiterate that the morphology of the cavities does not appear to change after long-time annealing (e.g., see Fig. 9).

Finally, Fig. 10 summarizes the various stages in the progress towards thermodynamic equilibrium of a system consisting of an implanted metal source in close proximity to disorder or cavities, which provide strong interstitial sinks. The implanted metals are initially supersaturated within a highly disordered region of Si (solid curve in Fig. 10). In the first (transient) stage for short-time annealing, the metals are rapidly redistributed (through rapid interstitial diffusion) to the disorder or strong sinks presented by a cavity band without appreciably dissolving into the bulk (dashed curve in Fig. 10). In such cases, we suggest a pseudoequilibrium in which the amount of metals in solution in these wafers is well below the level expected for thermodynamic equilibrium in the absence of disorder or cavities. However, the release of the metals from disorder or cavities can be limited by various processes such as strong trapping of metals to defects and cavity walls, the stability of defects and the availability of Si interstitials to mediate transport and/or dissolution of metal silicides. As a result of such metal-atom defect interactions, the system may be slow to reach thermal equilibrium (dotted curve) even for very fast interstitial diffusers such as Cu. This slow equilibration may mean that the system never attains thermodynamic equilibrium under normal Si processing times.

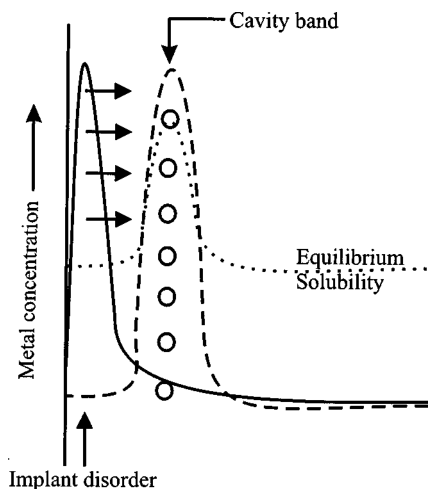

FIG. 10. Schematic summarizing the sequence of events in the gettering of implanted metals to cavities.

In conclusion, a high-implanted concentration of Cu and Au can be relocated from the near surface to a band of nanocavities during annealing with concentrations of metallic impurities in the bulk of the wafer far below the equilibrium solubility levels. This (transient) gettering process, despite appearing to be metastable, may be useful in removing metal impurities from active device regions when the annealing time is insufficient to achieve thermodynamic equilibrium. For longer annealing times at appropriate temperatures, the system slowly progresses towards equilibrium determined by the thermodynamics of the system.

[1] E. R. Weber, Appl. Phys. A: Solids Surf. **30**, 23 (1983).

[2] W. Schröter, M. Seibt, and D. Gilles, *Electronic Structure and Properties of Semiconductors*, Vol. 4 of *Materials Science and Technology: a Comprehensive Treatment* (VCH Weinheim, New York 1991), p. 575.

[3] *The National Technology Roadmap for Semiconductors* (Semiconductor Industry Association, San Jose, California, 1994).

[4] F. C. Frank and D. Turnbull, Phys. Rev. **104**, 617 (1956).

[5] U. Gösele, W. Frank, and A. Seeger, Appl. Phys. **23**, 361 (1980).

[6] N. A. Stolwijk, J. Hölzl, W. Frank, E. R. Weber, and H. Mehrer, Appl. Phys. A: Solids Surf. **39**, 37 (1986).

[7] J. Hauber, N. A. Stolwijk, L. Tapfer, H. Mehrer, and W. Frank, J. Phys. C **19**, 5817 (1986).

[8] N. A. Stolwijk, J. Hölzl, W. Frank, J. Hauber, and H. Mehrer, Phys. Status Solidi A **104**, 225 (1987).

[9] J. Wong-Leung, C. E. Ascheron, M. Petravić, R. G. Elliman, and J. S. Williams, Appl. Phys. Lett. **66**, 1231 (1995).

[10] S. A. Chambers and J. H. Weaver, J. Vac. Sci. Technol. A **3**, 1929 (1985).

[11] J. Wong-Leung, E. Nygren, and J. S. Williams, Appl. Phys. Lett. **68**, 416 (1995).

[12] S. Coffa, N. Tavolo, F. Frisina, G. Ferla, and S. U. Campisano,

Nucl. Instrum. Methods Phys. Res. B **74**, 47 (1993).
[13] A. Cros, J. Derrien, and F. Salvan, Surf. Sci. **110**, 471 (1981).
[14] D. M. Follstaedt, Appl. Phys. Lett. **62**, 1116 (1993).
[15] M. Gao, X. F. Duan, F. Wang, and J. Li, Appl. Phys. Lett. **72**, 2544 (1998).
[16] J. Wong-Leung, *et al.*, in *Proceedings of the Tenth International Conference on Ion Implantation Technology*, *Catania, Italy*, 1994 [Nucl. Instrum. Methods Phys. Res. B **96**, 253 (1995)].
[17] S. M. Myers and G. A. Petersen, Phys. Rev. B **57**, 7015 (1998).
[18] G. Bronner and J. Plummer, J. Appl. Phys. **61**, 5286 (1987).
[19] J. Wong-Leung, J. S. Williams, and M. Petravić, in *Defects and Diffusion in Silicon Processing*, edited by T. D. de la Rubia, S. Coffa, P. A. Stolk, and C. S. Rafferty, MRS Symposia Proceedings No. 469 (Materials Research Society, Pittsburgh, 1997), p. 457.
[20] S. M. Myers, D. M. Follstaedt, and D. M. Bishop, *Proceedings of the 17th International Conference on Defects in Semiconductors* [Mater. Sci. For. **143-147**, 1635 (1994)].
[21] N. A. Stolwijk, B. Schuster, and J. Hölzl, Appl. Phys. A: Solids Surf. A**33**, 133 (1984).